For conventional OFDM, the sampling factor for all the subchannels is the same and the ISI and ICI can be found simply by replacing the n_j and n_k in eqns. 4*a* and 4*b*, respectively, by the number of subchannels, M. Numerical analysis shows that the performance of the conventional OFDM and the wavelet-based MC scheme is the same for additive white Gaussian noise.

Performance: Simulations were carried out to compare the level of interference of the two MC transmission schemes over a two-path wireless channel (p = 1). The ISI and ICI power for each of subchannels were obtained and the mean value of interference calculated. Fig. 2 shows that, compared with conventional OFDM, the average ICI power in the case of the wavelet is vastly reduced. It can be seen that the ICI can be significantly reduced by increasing the length of the QMF, although this is accompanied by a small increase in the ISI power, as shown in Fig. 3. Referring to Figs. 2 and 3, some wavelets, such as wavelets derived from a Daubechies filter with length six, vastly reduce the power of ICI with almost the same performance in the ISI power when compared with conventional OFDM. Note also that, as the number of carriers increases, the ICI power is reduced dramatically for the wavelet-based MC system. Table 1 shows that the orthonormal wavelets derived from Haar QMFs perform well in reducing both the ISI and ICI power when compared to conventional OFDM.

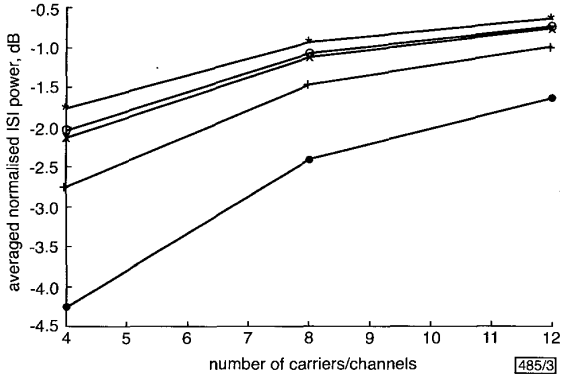

Fig. 3 *Averaged normalised ISI power for conventional and wavelet-based OFDM*

—○— conventional OFDM
—◆— wavelet-based - Haar
—+— wavelet-based - Daubechies-4
—×— wavelet-based - Daubechies-6
—✳— wavelet-based - Daubechies-8

Table 1: Averaged normalised power of interference for MC transmission

Conventional OFDM	ISI_{av} [dB]	–1.07	–0.72	–0.54
	ICI_{av} [dB]	–6.60	–8.16	–9.31
Wavelet-based MC transmission wavelets derived from Haar QMFs	ISI_{av} [dB]	–2.41	–1.62	–1.23
	ICI_{av} [dB]	–7.49	–12.94	–18.67
Channel excess delay		T	T	T
Number of carriers		8	12	16

Conclusions: The Daubechies and Haar wavelet-based MC transmission over a two-path channel has been addressed and the performance of the technique, in terms of ISI and ICI power, has been investigated. Simulation results have demonstrated that, compared with the conventional OFDM, the ICI power is significantly, and the ISI power slightly, reduced.

2 August 2000
Electronics Letters Online No: 20001263
DOI: 10.1049/el:20001263

B.G. Negash and H. Nikookar (*International Research Centre for Telecommunications-Transmission and Radar (IRCTR), Faculty of Information Technology and Systems, Delft University of Technology, P.O. Box 5031, 2600 GA Delft, The Netherlands*)

E-mail: H.Nikookar@ITS.TUDelft.NL

References

1 VETTERLI, M., and KOVACEVIC, J.: 'Wavelets and subband coding' (Prentice Hall PTR, Englewood Cliffs, New Jersey, 1995)
2 VAIDYANATHAN, P.P.: 'Multirate systems and filter banks' (Prentice Hall PTR, Englewood Cliffs, New Jersey, 1993)
3 NIKOOKAR, H., and PRASAD, R.: 'Multicarrier transmission with nonuniform carriers in a multipath channel'. Int. Conf. Universal Personal Communications, ICUPC'96, Boston, MA, USA, September 1996, pp. 628–632

160Gbit/s wavelength shifting and phase conjugation using periodically poled $LiNbO_3$ waveguide parametric converter

I. Brener, B. Mikkelsen, G. Raybon, R. Harel, K. Parameswaran, J.R. Kurz and M.M. Fejer

High efficiency 160Gbit/s wavelength conversion and optical phase conjugation using cascaded nonlinearities in periodically poled $LiNbO_3$ waveguides is reported. The authors also report on use of this device as a dispersion compensator for transmission of 100Gbit/s OTDM data through 160km of singlemode fibre.

Introduction: Wavelength conversion independent of modulation format and bit rate will play an important role in future transparent optical networks. Among all the techniques used in the past, parametric wavelength conversion is the only one that can satisfy these transparency requirements. Four-wave mixing (FWM) in nonlinear fibres, semiconductor optical amplifiers or nonlinear waveguides [1] as well as difference frequency mixing in nonlinear waveguides [2] have been used in the past for high speed wavelength conversion. Recently, we have shown that using a cascaded $\chi^{(2)}$ process in optimised periodically poled $LiNbO_3$ (PPLN) waveguides [3] enables high conversion efficiency (better than –10dB fibre to fibre) to be achieved while preserving all the advantages of a parametric processes. Furthermore, this parametric wavelength conversion is accompanied by phase conjugation. These high-speed phase conjugator devices can be used for compensation of dispersion and fibre nonlinearities [3, 4].

In this Letter we explore the performance of cascaded $\chi^{(2)}$ PPLN waveguide converters in high speed OTDM transmission, and show that these devices can perform penalty-free wavelength conversion of ~60–70nm at data rates up to 160Gbit/s. These data rates are well above those demonstrated using devices based on carrier dynamics, and thus make PPLN wavelength converters suitable for future high speed OTDM transmission.

Experiment: The devices used in this work are 6.5cm long and are fabricated using electric field poling of $LiNbO_3$ followed by annealed proton exchange. The details of the fabrication are described elsewhere [3]. The waveguides include input and output taper sections that improve the fibre coupling efficiency. Their typical fibre-to-fibre loss lies between 3 and 4dB. In the cascaded $\chi^{(2)}$ configuration, a pump and signal (both in the 1550nm wavelength region) are combined in a fibre coupler and launched into the waveguide. Two simultaneous processes take place inside the waveguide: (i) frequency doubling of the pump from a frequency ω_p to $2\omega_p$; (ii) difference frequency mixing between the doubled pump at $2\omega_p$ with the channel at ω_s yielding a shifted channel at $2\omega_p - \omega_s$. This process mimics FWM but with a much higher efficiency than that of FWM in fibre.

The setup used is shown in Fig. 1*a*. A 160Gbit/s bit-stream is generated by optical multiplexing of eight uncorrelated 20Gbit/s RZ signals (PRBS = 2^{31}–1), realised by an electro-absorption (EA) modulator based pulse carver followed by an $LiNbO_3$ data modulator [5]. The signal is combined with the pump (provided by an amplified tunable laser) and then launched into the PPLN waveguide. After the waveguide, the remaining pump is rejected with a fibre grating and the converted signal is further filtered and amplified in another EDFA. In the 160Gbit/s optically pre-amplified receiver, optical demultiplexing and clock recovery are achieved using EA modulators. Although the 160Gbit/s data is

assembled using a TDM rate of 20Gbit/s, the demultiplexer operates at 10GHz in order to eliminate an additional electronic demultiplexer necessary for BER measurements.

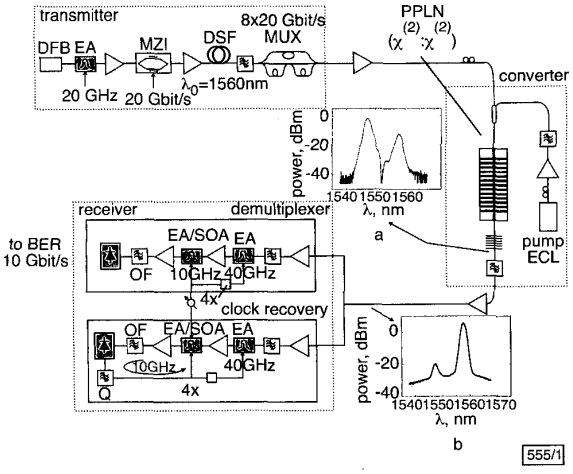

Fig. 1 *Schematic diagram of experimental setup consisting of OTDM transmitter and receiver, and PPLN waveguide wavelength converter*

Insets: Resulting optical spectra at two points after the wavelength converter, where the original and converted channels are visible

The insets in Fig. 1 show the optical spectra measured at different points after the PPLN wavelength converter. Inset *a* shows the spectra immediately after the grating, where the only visible features are the original OTDM channel (left peak) and the converted channel (right peak) at a spacing of 10.8nm. The pump wavelength was 1552.5nm but it is not visible in the inset due to the filtering performed by the fibre grating (better than 40dB). To suppress the original channel at 1547.15nm, we inserted a tunable filter tuned to the converted channel at 1558nm. Inset *b* in Fig. 1 shows the resulting optical spectra. The filter narrows the spectral width of the converted channel from 1.86 to 1.5nm (FWHM), but this did not cause any appreciable penalty even at a bit rate of 160Gbit/s.

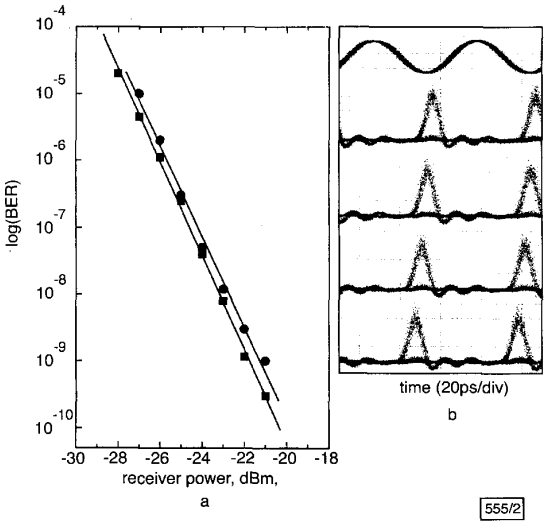

Fig. 2 *Transmission performance and eye diagrams*

a Transmission performance of wavelength converter (with no fibre) at 160Gbit/s
BER traces are shown for a typical sub-channel in the OTDM train
● back-to-back
■ converted
b Some of the demultiplexed eye diagrams measured at the receiver

Fig. 2*a* shows the BER performance of one of the demultiplexed sub-channels in the wavelength-converted channel compared to a back-to-back measurement. A very small improvement of ~0.7dB was observed, although this is very close to the experimental error bar (~0.5dB). Similar BER curves were measured in all 16 subchannels. Fig. 2*b* shows the eye diagrams of a few of the optically demultiplexed OTDM channels; a fully open eye was observed for all of the sub-channels.

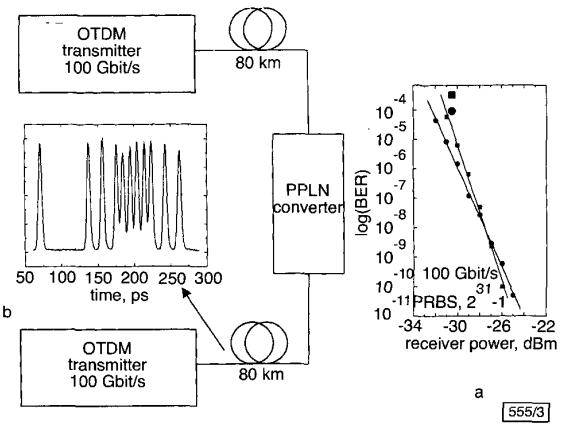

Fig. 3 *Performance of PPLN device used as dispersion compensator at 100Gbit/s and using two 80km fibre spans (D = 5ps/nm.km)*

a BER traces
■ back-to-back
● converted
PRBS, 2^{31}–1
b Typical bit sequence at the receiver

Finally, in Fig. 3 we show the performance of this wavelength converter as a dispersion compensator when used between two 80km fibre spans (D = 5ps/nm km). The bit rate was then reduced to 100Gbit/s (dispersion compensation at 160Gbit/s using phase conjugation was not possible due to third-order dispersion). Although phase conjugation cannot correct for third-order dispersion, we measured a penalty of less than 0.5dB at the receiver with no extra dispersion-compensating fibre. Inset shows an example of a bit sequence of the converted channel measured using a streak camera.

Conclusion: We have demonstrated high efficiency wavelength conversion and phase conjugation through a PPLN waveguide at a line rate of 160Gbit/s. The same device was used successfully for dispersion compensation through 160km of fibre at 100Gbit/s. These experiments show the suitability of this family of parametric wavelength converter devices for line rates in excess of 80Gbit/s.

3 August 2000
Electronics Letters Online No: 20001264
DOI: 10.1049/el:20001264

I. Brener, B. Mikkelsen, G. Raybon and R. Harel (*Bell Laboratories, Lucent Technologies, 600 Mountain Ave., Murray Hill, NJ 07974, USA*)

E-mail: ibrener@tellium.com

K.R. Parameswaran, J.R. Kurz, M.M. Fejer (*E.L. Ginzton Laboratory, Stanford University, Stanford, CA 94305-4085, USA*)

I. Brener: Currently at Tellium Inc., PO Box 901, 2 Crescent Pl., Oceanport, NJ 07757, USA

References

1 YOO, S.J.B.: 'Wavelength conversion technologies for WDM network applications', *IEEE J. Lightwave Technol.*, 1996, **14**, pp. 955–966

2 CHOU, M.H., HAUDEN, T., ARBORE, M.A., and FEJER, M.M.: '1.5-μm-band wavelength conversion based on difference-frequency generation in $LiNbO_3$ waveguides with integrated coupling structures', *Opt. Lett.*, 1998, **23**, pp. 1004–1006

3 CHOU, M.H., BRENER, I., FEJER, M.M., CHABAN, E.E., and CHRISTMAN, S.B.: '1.5-μm-band wavelength conversion based on cascaded second-order nonlinearity in $LiNbO_3$ waveguides', *IEEE Photonics Technol. Lett.*, 1999, **11**, pp. 653–655

4 BRENER, I., MIKKELSEN, B., ROTTWITT, K., BURKETT, W., RAYBON, G., STARK, J.B., PARAMESWARAN, K., CHOU, M.H., FEJER, M.M., CHABAN, E.E., HAREL, R., PHILEN, D.L., and KOSINSKI, S.: 'Cancellation of all Kerr nonlinearities in long fiber spans using a $LiNbO_3$ phase conjugator and Raman amplification'. Optical Fiber Conf., Baltimore, 2000, Paper PD 33

5 MIKKELSEN, B., RAYBON, G., ESSIAMBRE, R.J., JOHNSON, J.E., DREYER, K., and NELSON, L.F.: 'Unrepeatered transmission over 150km of nonzero-dispersion fibre at 100Gbit/s with semiconductor based pulse source, demultiplexer and clock recovery', *Electron. Lett.*, 1999, **35**, pp. 1866–1868

10Gbit/s RZ transmission over 5000km with gain-clamped semiconductor optical amplifiers and saturable absorbers

Z. Bakonyi, G. Onishchukov, C. Knöll, M. Gölles and F. Lederer

By combining a gain-clamped semiconductor optical amplifier (GC-SOA) and a saturable absorber-semiconductor optical amplifier module, 10Gbit/s RZ transmission over 5000km (200 × 25km) has been demonstrated in a fibre loop setup. It is shown that a GC-SOA could compensate for the patterning introduced by a conventional SOA.

In semiconductor optical amplifier (SOA) based transmission systems operating in IM-DD transmission mode the system performance is mainly limited by the fast accumulation of in-space noise. Traditionally, the noise upgrowth is reduced by using in-line bandpass filters and by gain map optimisation [1, 2]. In [3] we showed that by using saturable absorbers the problem of in-space noise upgrowth can be eliminated, and a 5Gbit/s RZ transmission over 30,000km was demonstrated in a fibre loop setup. The main reason for the unsatisfactory 10Gbit/s performance was strong patterning originating from the slow gain recovery time of the SOAs used. If the required gain for the 10GHz component of the signal was provided, the suppression of in-space noise was impossible [4].

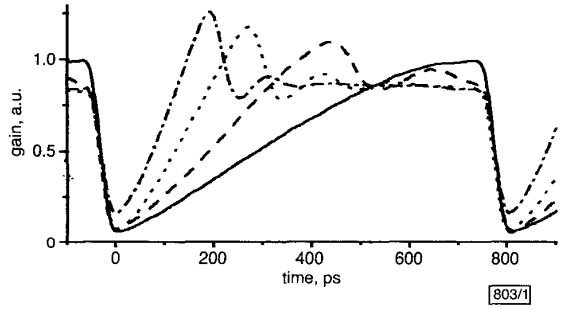

Fig. 1 *Gain recovery dynamics of gain-clamped SOA at different operating currents*

Driving current:
——— 70mA
– – – – 100mA
····· 150mA
–·–·– 250mA
In all cases the chip temperature is 20C°, pump wavelength is 1300nm and probe wavelength is 1310nm. Clamping laser wavelength is 1285nm, pump pulse energy is 0.6pJ and probe pulse energy is 0.3fJ.

Gain-clamped semiconductor optical amplifiers (GC-SOA) are generally considered to be an effective tool to address patterning suppression, although their high bit rate operation is limited by the relaxation oscillations of the clamping laser. We carried out pump-probe measurements to determine the gain recovery characteristics of a GC-SOA provided by JDS-Uniphase. A 1.25GHz train of 20ps pulses was applied as the pump and a train of 1.5ps pulses was used as the probe at a 10nm shifted wavelength. The measurement was based on beating the two pulse trains with slightly different (~10kHz) pulse repetition rates. Fig. 1 shows typical results of such measurements for the GC-SOA. It was found that the time needed to reach the first oscillation peak after saturation (rise-up time) as well as the relaxation oscillation frequency and the damping constant are tunable by the driving current, the input pulse power and the device temperature. Such gain relaxation dynamics are not always disadvantageous and can be utilised to compensate for the patterning introduced by the conventional SOA section of the SA-SOA module.

The scheme was tested in fibre loop experiments. The schematic layout of the experimental set up is presented in Fig. 2. It is identical to the one used in [3] except that a GC-SOA was applied as an additional in-line amplifier instead of a conventional MQW-SOA. The saturable absorber section of the combined module was created by ion implantation and can be characterised by a ~30ps recovery time and 3dB transmission bleaching. The additional amplifier is required since the overall fibre-to-fibre gain of the SA-SOA module is about unity. As was shown in [3, 4] the energy of the injected data pulses quickly attains a steady state value. Once the bit slot duration is reduced, the stable energy of the data pulses becomes increasingly bit pattern dependent since the amplifier gain cannot fully recover between the pulses. If the data pulses succeed each other too rapidly, the gain of the amplifier is substantially reduced and, accordingly, the pulse energy and the absorber saturation are likewise reduced. This results in a net loss, the pulses become unstable and after several round trips each second pulse is omitted.

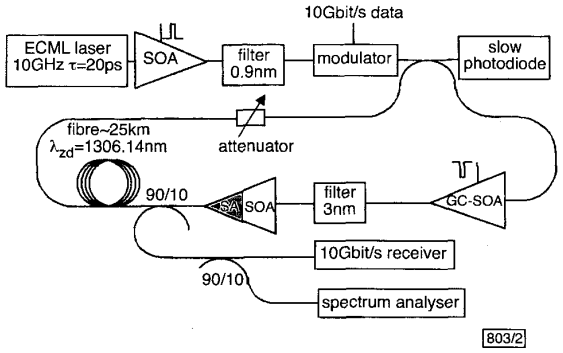

Fig. 2 *Recirculating fibre loop setup*

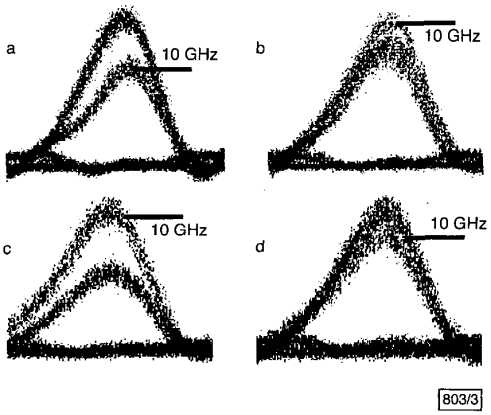

Fig. 3 *Eye diagrams of 10Gbit/s '111011101010' bit train after eight round trips (200km)*

Amplifier currents:
a 70mA
b 90mA
c 110mA
d 200mA
Value of the input pulse energy is ~0.05pJ
10GHz component of signal is marked

The steady state energy levels in the system containing the GC-SOA were studied by a bit sequence, which had only 5 and 10GHz pulse repetition rate components. At low current below the lasing threshold, the GC-SOA acts as a conventional SOA and the 10GHz signal component has a lower energy (Fig. 3*a*). When the current is increased, the first peak of the relaxation oscillation moves forward and the 10GHz component is situated at the leading edge of the first oscillation and the 5GHz component is at the trailing edge (Fig. 3*b*). By further increasing the current, a very strong inverse patterning could be obtained, as is shown in Fig. 3*c*. This corresponds to the situation where the 10GHz component is around the first peak of the relaxation oscillations and the 5GHz component is at the dip. In Fig. 3*d* the 10GHz component succeeds the first peak and the excess gain in the GC-SOA